THE HIPPARCOS SOLAR SYSTEM OBJECTS ANNEXES

D. Hestroffer

Astrophysics Division, ESTEC, NL-2200AG Noordwijk, The Netherlands

ABSTRACT

Astrometric and photometric measurements of a number of solar system objects were performed by the Hipparcos satellite in both the Hipparcos main mission and the Tycho experiment. The specific aspects of the Hipparcos observations and reduction process implemented for the solar system objects are presented. Special attention is paid to the error budget of the reduction which is accurate to the mas (milliarcsecond) level for the Hipparcos main mission. The contents of the Hipparcos Solar System Objects Catalogues is described. Comparison between the results derived from the two Consortia FAST and NDAC, as well as comparison with ground-based observations, are given.

Key words: Astrometry, photometry, solar system.

1. INTRODUCTION

Among the thousands of stars, the Hipparcos programme included a selection of solar system objects (major planets, planetary satellites and asteroids). The primary motivation is to provide highly accurate positions for the link of the dynamical reference system to the International Celestial Reference System (ICRS), but also to enable dynamical and physical studies of these objects. The value of astrometric observations of asteroids, relatively to the reference frame defined by the stars, for the establishment of the dynamical reference frame, was first suggested by Dyson (1928). These objects were thought to considerably enhance the results obtained from observations of the Sun or major planets. Nonetheless, this method encountered some limitations; hence such observations of minor planets enter for instance in the solution derived by Fricke (1982) for the FK5 with a relatively modest weight. Hipparcos should dramatically improve the situation (e.g. Hestroffer et al. 1995; Bec-Borsenberger et al. 1995), and yield a link between the dynamical system and the ICRS with a precision of the same order of magnitude as the best result obtained so far (Folkner et al. 1994).

High precision measures of the positions of asteroids enables to improve their ephemerides but also in particular cases of very close encounters to determine the mass of some of them (e.g. Viateau 1997; Bange & Bec-Borsenberger 1997). The observations of planetary satellites relative to the background stars yield, in an indirect manner, accurate positions of the gravitating major planet's centre of mass (Morrison et al. 1997; Fienga et al. 1997). Photometric observations of asteroids provides information about their rotational properties such as shape and spin-vector orientation, and the scattering properties of their surface. Hence observations of such primordial objects yield insight on their collisional evolution, and on the early solar system.

The Hipparcos satellite successfully observed the solar system objects during its almost 4 years mission duration. Hence it provides astrometric as well as photometric information on these relatively bright objects. The retained objects and the geometry of the Hipparcos observations are briefly presented in Section 2. The information gathered by the star mapper constitutes the Tycho Catalogue, while the Hipparcos Catalogue is derived from the observations made through the main grid. The reduction of the solar system objects observations follows the procedure retained for the stars on the first stages, and is adapted to these rapidly moving and eventually resolved objects. The data are of different nature and precision and are presented separately in Sections 3 and 4. All astrometric positions are given in the ICRS, and the transformation is presented in Section 5. Comparison with ground-based observations and calculated places, and between the NDAC and FAST positions, are given in Section 6.

2. HIPPARCOS OBSERVATIONS

2.1. Observing Programme

Initially two satellites (Europa and Titan) and 63 asteroids were retained in the Hipparcos (main mission) programme. Positions of the solar system objects were entered in the Input Catalogue by means of their ephemerides (Bec-Borsenberger 1985). Since the positions had to be known *a priori* with a precision better than 1 arcsec, a ground-based campaign of observations of these asteroids was started in 1983 in order to improve the accuracy of their ephemerides. The number of retained asteroids was reduced to 48 after consideration of the number of their predicted transits during the scheduled nominal mission duration. The Saturnian satellite S8 Iapetus was added

to the observation programme during the mission. *A priori* ephemerides of the 48 Hipparcos asteroids, the four Galilean satellites, Titan, Venus and planets Mars through Neptune were also calculated as part of the Tycho Input Catalogue of 3 million stars. Nevertheless, not all of these solar system objects were retained for the Catalogue output (see Section 3); their inclusion was necessary for technical reasons (Bastian & Wagner 1997).

2.2. A Scanning Satellite

Since the Hipparcos satellite was scanning the whole sky in a regular manner, no pointing to a specific object was possible; but an observation occurred during its transit across the field of view. Moreover the spin axis of the satellite was precessing with a constant angle of 43° around the direction towards the Sun, enabling a complete and optimal coverage of the celestial sphere. On the other hand, solar system objects are gravitating around the Sun in a band near the ecliptic, thus observations of these objects are spread around the quadratures (see Figure 1), i.e. when the solar phase angle is maximal. Also the total number of observations is varied between the different observed objects (from roughly 15 to 125 transits). The same remark applies for the distribution of these transits in time or along the planet's trajectory. The Hipparcos and Tycho observations are of course almost simultaneous; a transit across the star mapper occurs a few seconds before the transit across the main grid.

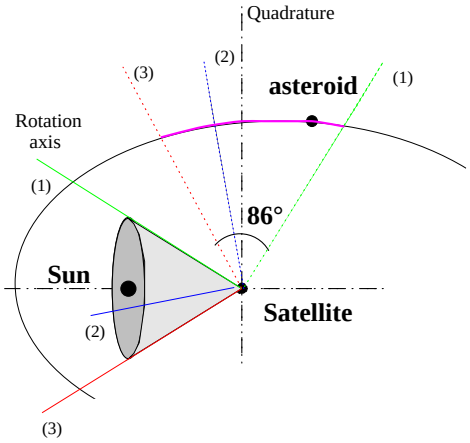

Figure 1. Schematic view of the Hipparcos satellite's scanning law. The observations of solar system objects are made around the quadratures.

3. TYCHO

The data gathered by the star mapper constitute the Tycho Catalogue. A schematic view of the grid system is given in Figure 2. The Tycho observations are not adapted to objects larger in apparent size than the smallest separation between two slits (5.63 arcsec). At least for this reason no data can be provided for Venus, Mars, Jupiter and Saturn. Next, the objects brighter than $V \sim 10$ and with sufficient number of observations were retained; the list is given in Table 1. When available, the photometry is provided in the Tycho B_T and V_T passbands which, although not identical, are close to the Johnson B and V. Over the range $-0.2 < (B-V)_T < 1.8$, the following linear formulae yield transformations between the two photometric systems accurate to 0.05 mag:

$$V_T - V_J = 0.09\,(B-V)_T$$
$$(B-V)_J = 0.85\,(B-V)_T$$

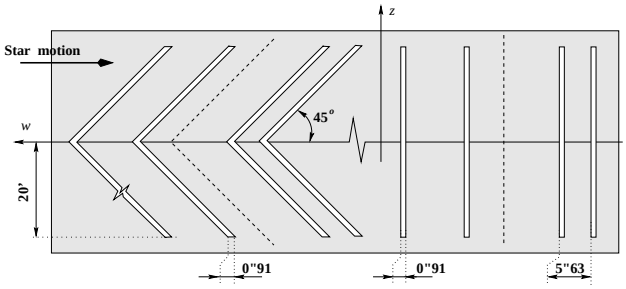

Figure 2. Schematic view of the star mapper slits system. All slits have the same width in the direction of the w axis. The inclined and vertical slits are spaced, in the direction of a star's motion, with distance ratio 2:3:1 of the step s = 5.63 arcsec. The 'fiducial lines', which can be thought as the centres of gravity of the four slits in each group, are shown as dashed lines.

Table 1. Solar system objects of the Tycho Catalogue.

Name	Photometry	Astrometry
Minor planets:		
(1) Ceres	√	√
(2) Pallas	√	√
(4) Vesta	√	√
(6) Hebe	√	√
(7) Iris	√	√
Satellites:		
J III–Ganymede	–	√
J IV–Callisto	–	√
S VI–Titan	√	√
Major planets:		
Uranus	–	√
Neptune	–	√

The magnitudes in the two channels are derived, in the same way as for the stars, from the amplitude of the convolved signal and are calculated by a simplified calibration procedure. The magnitude provided for each transit corresponds to the mean of the measure for each slits group crossing. No magnitude is provided for objects larger in apparent size than the width of the slits (0.91 arcsec). For objects that were not substantially smaller than the slit's width, systematic errors may occur. Finally, no standard errors are provided for the estimation of the B_T and V_T

magnitudes; they are of the order of 0.1 mag for an object of magnitude $V \sim 8$ and 0.35 mag for $V \sim 10$.

Since the transits across each slits group yield information in two directions, one can derive a conventional two-dimensional position on the celestial sphere for each transit. The displacement of the solar system object between the crossing of the fiducial lines of the slit groups (in a time interval up to about 10 s) is known with sufficient accuracy to enable such a construction. The primary astrometric information is the time when an object crosses the fiducial line as derived in the detection and estimation process. The difference between the observed and predicted crossing time for each slit group is converted into an along-scan residual on position. Next the two along-scan residuals (Δu_1, Δu_2) are transformed into residuals in the two orthogonal directions w and z associated to the focal plane of the telescope. This transformation $\mathbf{P}$ depends on the sign of the z coordinate, whether the transit occurs in the upper part ($\mathrm{sgn}(z) = +1$) or the lower part ($\mathrm{sgn}(z) = -1$) of the inclined slits. The orientation of the (w, z) frame on the celestial sphere is given by the position angle θ. The observed position, at the—arbitrarily chosen—reference epoch t_2, is thus derived from an *a priori* calculated position (close to the true position) and the along-scan residuals by:

$$\begin{pmatrix} \Delta\alpha_2 * \\ \Delta\delta_2 \end{pmatrix} = \mathbf{R}_{(\theta)}\ \mathbf{P}\ \begin{pmatrix} \Delta u_1 \\ \Delta u_2 \end{pmatrix} \qquad (1)$$

where $\Delta\alpha* = \Delta\alpha \cos\delta$, and where:

$$\mathbf{R}_{(\theta)} = \begin{pmatrix} \sin\theta & -\cos\theta \\ \cos\theta & \sin\theta \end{pmatrix}$$

$$\mathbf{P} = \begin{pmatrix} 0 & 1 \\ \mathrm{sign}(z) & -\mathrm{sign}(z) \end{pmatrix}$$

The second-order terms arising from the transformation between the tangent plane and the celestial sphere are neglected. Introducing the diagonal matrix of the standard error of the measurements:

$$\sigma = \begin{pmatrix} \sigma_1 & 0 \\ 0 & \sigma_2 \end{pmatrix}$$

the variance matrix of the derived coordinates is given by:

$$\begin{pmatrix} \sigma^2_{\alpha*} & \sigma_{\alpha*}\,\sigma_\delta\,\rho^\delta_{\alpha*} \\ \sigma_{\alpha*}\,\sigma_\delta\,\rho^\delta_{\alpha*} & \sigma^2_\delta \end{pmatrix} = \mathbf{R}_{(\theta)}\ \mathbf{P}\ \boldsymbol{\sigma}^{\mathbf{2}}\ \mathbf{P}'\ \mathbf{R}'_{(\theta)}$$

This matrix is no longer diagonal, reflecting the fact that—depending on the position angle θ and the ratio σ_1/σ_2—the principal axis of the associated error ellipse does not coincide with the (N,E) directions toward the northern celestial pole and the east. The along-scan standard errors are derived from an error model adequate for stellar images and do not correspond to a Gaussian noise. Moreover, the signals for planets are broader and more flat at the top than the signals of point-like sources. Thus the derived quantities $\sigma^2_{\alpha*}$ and σ^2_δ should preferably be regarded as indicators of the quality of a single measure.

For each transit, the astrometric observation is defined by the reference epoch t_2, the coordinates (α, δ), the standard errors $\sigma_{\alpha*}$, σ_δ and the correlation between the two coordinates $\rho^\delta_{\alpha*}$. To enable future systematic correction of the data, especially for the large major planets, the position angle θ, the inclined-slit flag sign(z), and the standard errors σ_1, σ_2 are provided as additional data. All positions are referred to the ICRS system (see Section 5). It is stressed that phase, shape or albedo corrections are not taken into account. The position corresponds to the photocentre for the smallest objects. For Uranus, Neptune and to a lesser extent the two Jovian satellites, whose angular diameters are larger than the slit width, the position on the surface of the body depends highly on its albedo distribution and the scanning geometry. More accurate correction to the centre of figure can be applied by a simulation of the Tycho photon counts and convolution with the slit response. A general description of the procedure to follow is given in the Hipparcos Catalogue (Høg & Makarov 1997).

4. HIPPARCOS

In contrast to the star mapper, the main grid is made of 'vertical' slits, and hence only provides a one-dimensional position, i.e. the observed position locus in the direction perpendicular to the slits. Astrometry is provided for objects brighter than $V \sim 13$ and smaller in apparent size than $\rho \sim 1$ arcsec, i.e. 48 asteroids, the planetary satellites J2 Europa, S6 Titan and S8 Iapetus (unfortunately only a very few observations are available for Iapetus).

The primary astrometric and photometric information is obtained from the Fourier expansion of the modulated signal:

$$S(t) = I\,[1 + M\,\cos(\omega\,t + \varphi) + N\,\cos(2\omega\,t + 2\psi)] \qquad (2)$$

where ω is the fundamental angular frequency. This reduces for a point-like source to:

$$S(t) = I\,[1 + M_o\,\cos(\omega\,t + \varphi_o) + N_o\,\cos(2\omega\,t + 2\varphi_o)] \qquad (3)$$

where M_o, N_o are calibrated modulation coefficients, and the modulation phases are independent of the harmonic rank ($\varphi = \psi = \varphi_o$). The astrometry is given at this stage by an abscissa v as derived from the modulation phases φ, ψ within FAST, and the phase φ, of the first harmonic only, within NDAC. For a point-like or relatively small source (typically with a diameter $\rho \lesssim 0.05$ arcsec), the FAST and NDAC abscissae have the same expectancy since the calibrated phases φ and ψ are (almost) equal. For a larger extended source, the difference between the FAST and NDAC abscissa depends on the physical properties of the minor planet or planetary satellite (such as apparent diameter, solar phase angle, albedo distribution over the visible surface and scanning geometry).

In contrast to the stars, the FAST and NDAC solutions have not been merged into a single position. The FAST reduction procedure is not adapted to the

observations of the largest objects J2 Europa and S6 Titan, thus only the NDAC positions are provided. For smaller objects, both procedures are valid; but as noted before, the FAST and NDAC positions loci do not strictly speaking correspond to the same point on the surface of the object. Hence, in order to avoid introducing additional errors, no merging of the data was performed. Nevertheless, for the smallest bodies (relatively to the grid step), both FAST and NDAC loci correspond as a first approximation to the position of the photocentre (Hestroffer & Mignard 1997).

The displacement on the sky of an asteroid or a planetary satellite during the ~ 17 seconds it takes to cross the main grid, can be calculated with sufficient accuracy to enable the construction of a normal position locus for each transit. A linear regression is performed over the transit in order to determine the average offset between the calculated and observed abscissae. This offset is given by a weighted mean within NDAC (L2 fit) and by the median within FAST (L1 fit). The reference epochs, the standard error associated to these two estimators and the great circle on which the positions are projected are different.

The apparent positions are corrected for aberration, gravitational light bending by the Sun, and for the Hipparcos satellite's parallax (the geocentric position was provided with an accuracy of ~ 2 km by the satellite orbit determination performed at ESOC). The epoch of observation is also corrected for the first order light-time difference due to the geocentric orbit. Hence the published position corresponds to the astrometric direction at time $t - \tau$, where t is the published epoch of observation and τ is the light-time delay to the geocentre. The astrometric direction for each transit is supplied by means of a reference point (α_0, δ_0) and the direction of the straight line $v =$ constant in the tangent plane associated with this reference point (see Figure 3). The reference point is constructed in such a way that it has the same observed abscissa on the reference great circle, and a ordinate given by the calculated ephemeris. All positions are referred to the ICRS system (see Section 5), it is stressed that phase, shape or albedo corrections are not taken into account.

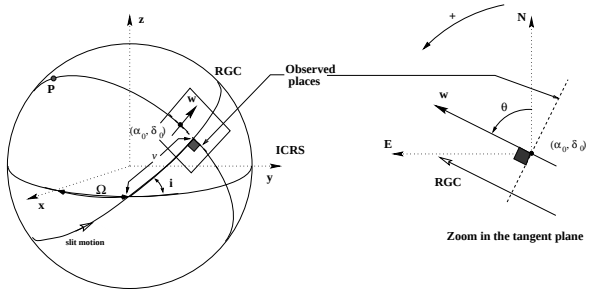

Figure 3. Reference point and transformation to the tangent plane.

The photometry is provided (only within FAST) for the 48 asteroids of the mission in the Hipparcos Hp broad-band photometric system. No photometry is available for the planetary satellites since the diffusion of the light of their respective planets perturbed considerably the measurements. Two estimators of the apparent magnitude ($Hp_{\rm dc}$ and $Hp_{\rm ac}$) are derived from the coefficients I, IM, IN. The apparent magnitude $Hp_{\rm dc}$ is directly given by the mean intensity I corrected for background noise. The second estimator $Hp_{\rm ac}$ is derived from the amplitude IM, IN of the modulation. It is stressed that the $Hp_{\rm ac}$ estimator, given as additional data, is of lower precision and biased. We have, in a first approximation, for a spherical object of apparent diameter ρ:

$$Hp_{\rm ac} - Hp_{\rm dc} \sim a\,\rho^2 + o\,(\rho^4) + o\,(\alpha)$$

where $a > 0$ is a scalar and α is the solar phase angle. The transformation from the Hp system to standard magnitudes are given by Mignard et al. (1997). The Hp and V_J bands have more or less the same effective wavelength, they can be related in a good approximation for solar system objects (with $-0.5 \lesssim B - V \lesssim 1.5$) by a relation involving the $B-V$ colour index in the Johnson system (Mignard, private communication):

$$\begin{aligned} Hp - V_J \quad \sim \quad & 0.304\,(B-V) - 0.202\,(B-V)^2 \\ & +0.107\,(B-V)^3 - 0.045\,(B-V)^4 \end{aligned}$$

The Hipparcos solar system objects photometric catalogue is completed, for convenience, with some additional calculated aspect data: the distance to the Sun, the distance to the satellite and the solar phase angle.

5. TRANSFORMATION TO THE ICRS

After the sphere reduction stage, all Hipparcos or Tycho solar system objects astrometric positions are related to intermediary reference frames P (called F37.3 for FAST, N37.5 for NDAC and for historical reasons N18 for TDAC). However the positions have to be given in the system of the final Hipparcos Catalogue, i.e. the optical counter part of the ICRS. All the reference frames P are defined by the stars and the associated sphere construction; they are related to the single sphere solution H37C (Lindegren et al. 1997). This latter reference frame is next aligned to the frame of the ICRS by a small time-dependent rotation (Kovalevsky 1997):

$$\boldsymbol{\varepsilon}(t) = \boldsymbol{\varepsilon}_0 + (t - T_0)\,\boldsymbol{\omega}$$

where $T_0 =$ J1991.25 is the reference epoch.

This rotation is accurate to 0.6 mas for the orientation and 0.25 mas/year for the spin components (Kovalevsky et al. 1997).

The Hipparcos astrometry of solar system objects is uni-dimensional. It is completely characterised by the abscissa and the orientation of the great circle on which the planet position is projected. Hence the published data determine the equation of the straight line $v =$ constant, in the tangent plane centred at the reference point (α_0, δ_0). The great circle is defined with respect to the stars and hence to the intermediary frame P. The origin for the abscissa of the position locus is at the ascending node of the great circle with the reference frame P. Thus the transformation to the ICRS is given by application of an infinitesimal

rotation to the reference point, the change on the position angle θ being negligible. The transformation for the Tycho and Hipparcos positions of solar system objects at epoch t is given by:

$$\mathbf{u}_{\rm ICRS}(\mathbf{t}) = \begin{pmatrix} 1 & \varepsilon_z(t) & -\varepsilon_y(t) \\ -\varepsilon_z(t) & 1 & \varepsilon_x(t) \\ \varepsilon_y(t) & -\varepsilon_x(t) & 1 \end{pmatrix} \mathbf{u}_{\rm P}(\mathbf{t})$$

where $\mathbf{u}_{\rm P}$ is the astrometric direction of either the Hipparcos reference point or the Tycho observed position:

$$\mathbf{u}_{\rm P} = \begin{pmatrix} \cos\alpha\cos\delta \\ \sin\alpha\cos\delta \\ \sin\delta \end{pmatrix}$$

For the Tycho data the spin components between the two reference frames are of the order of 1 mas/year and are negligible. Zonal and temporal systematic errors of larger size (up to 6 mas) were also neglected with regard to the random error of a single transit.

6. COMPARISONS AND PRECISIONS

The Tycho positions have some similarities to the coordinates obtained by meridian circles observations. The number of transits per apparition may however be considerably smaller, and since these occur around the quadratures, they are complementary to the ground-based measurements. Figure 4 shows the Hipparcos residuals obtained for Uranus with respect to the widely used DE200 ephemeris. These are given together with the residuals obtained with the Carlsberg instrument at La Palma (Morisson, private communication). Both observational data are in good agreement; in particular they show the systematic error in right ascension of the DE200 solution and the improvement obtained with the DE403 solution. It was noted in Section 3. that the precisions for Tycho observations are more indicative of the quality of the astrometric measures. As can be seen on the dispersion of the residuals, the Tycho positions are of the same order of precision than the ground-based observations carried out with vertical circles.

The FAST and NDAC astrometry have been obtained by independent means. They differ mainly by the fact that they have not been derived for the same epoch, neither do they correspond to projections on the same great circle, and as stated before, they do not correspond to the same point on the surface of the asteroid (see Section 4.). If we consider the subset of the 39 asteroids of size smaller than 0.2 arcsec[1], the correlation factor of 0.85 between the abscissae and the scaling of the standard errors as derived from faint stars (Arenou, private communication), we find the distribution of the normalised difference $\Delta v/\sigma_v$ given in Figure 5. As expected, this distribution is an almost centered Gaussian of unit variance (with a mean $\langle\Delta v\rangle < 1$ mas), so that no significant systematic offset is present between the FAST and NDAC positions for this subset of observations.

[1] Excluding the nine asteroids (1) Ceres to (7) Iris, (10) Hygiea and (324) Bamberga.

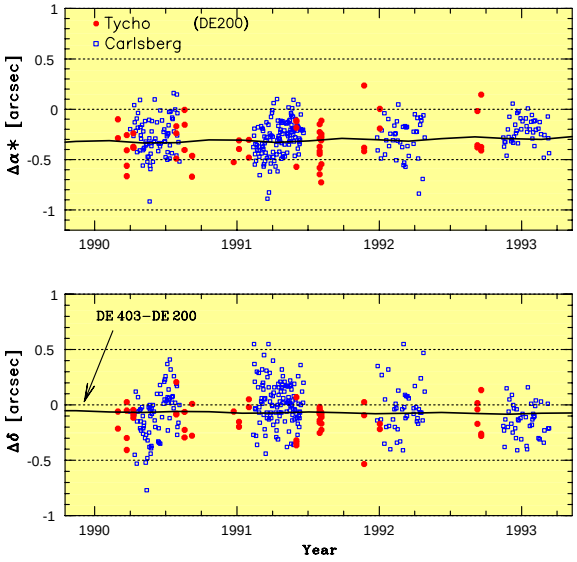

Figure 4. Residuals for the Tycho and Carlsberg positions of Uranus relative to the DE200 ephemeris. Each point corresponds to a single transit across each instrument.

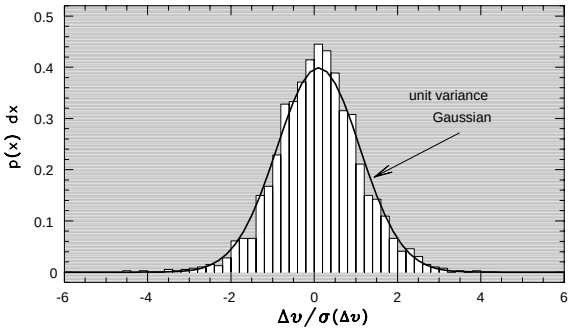

Figure 5. Normalised difference between the FAST and NDAC positions. The histogram is constructed from a subset of 39 minor planets and a total of 1967 transits in common to the NDAC and FAST catalogues.

The precision of the Hipparcos photometric and astrometric data at the transit level depend on the magnitude of the object at the observation epoch. The standard errors for the Hipparcos astrometry are given in Figure 6. With an average of $10-15$ mas, Hipparcos measures, which are directly related to the ICRS, surpass the ground-based meridian telescopes observations by a factor ~ 10. The average precision for the photometric dc component is $0.02-0.03$ mag. Since the dc and ac component are independent, a more precise estimator can be constructed by taking the (weighted) mean of the $Hp_{\rm ac}$ and $Hp_{\rm dc}$ values; it is however stressed that such a construction introduces systematic errors when the object's angular size is not negligible (i.e. when the modulation coefficients are such that $M > M_o$ and/or $N > N_o$, see Section 4).

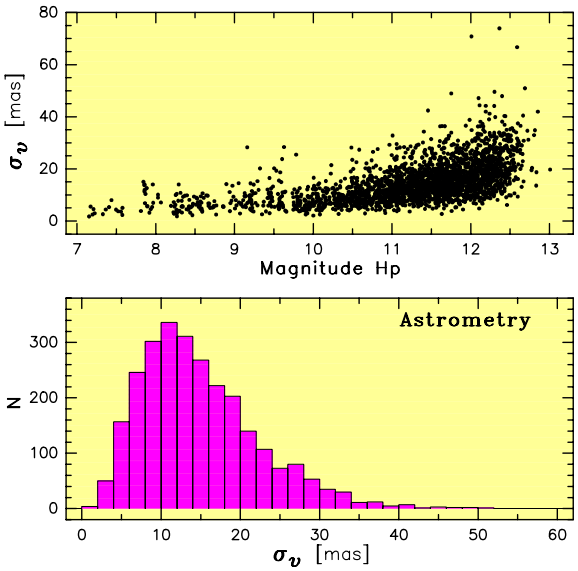

Figure 6. Standard errors for the Hipparcos astrometry σ_v as a function of apparent magnitude (top) and histogram (bottom). N is the number of transits.

7. CONCLUSION AND FUTURE PROSPECTS

The Hipparcos satellite provides valuable astrometric and photometric data for a total of 55 relatively bright solar system objects (mainly asteroids, but also planetary satellites and major planets). The observations are spread over the period ranging from the end of November 1989 to the mid of March 1993. The Tycho measures are of lower precision than the - main mission - Hipparcos ones, but are extended to larger objects. Tycho provides conventional astrometric positions in right ascension and declination, and photometry in two filters close to the Johnson B and V. Hipparcos provides one-dimensional astrometric positions, and photometry in the broad-band Hp photometric system. All astrometric positions are related to the ICRS. The results are gathered in the Hipparcos Solar System Objects Astrometric Catalogue, the Hipparcos Solar System Objects Photometric Catalogue, and the Tycho Astrometric and Photometric Catalogue. These appear in Volume 10 (printed format) of The Hipparcos and Tycho Catalogues (ESA 1997), and in the ASCII CD-ROMs (Volume 17).

As far as solar system objects are concerned, Hipparcos yields valuable information not only by direct observations of these objects, but also by the very accurate astrometric positions of reference stars in photographic plates or CCD (re-)reduction. Hipparcos also provides a strong basis for future astrometric missions. GAIA (Global Astrometric Interferometer for Astrophysics) proposed by Lindegren & Perryman (1996) within the the context of ESA's 'Horizon 2000 Plus' programme would allow astrometric observations on the sub-milli-arcsecond level of a few hundreds of small asteroids (Hestroffer & Morando 1995). It would also provide high precision photometry in a way similar to Hipparcos. In contrast to Hipparcos, GAIA would be able to resolve hundreds of asteroids (and also stars), leading for the first time to (1) the determination of their diameter in the optical domain, and (2) to a basis of comparison to the extensive results obtained in the IR domain by the IRAS satellite.

ACKNOWLEDGMENTS

The author is indebted to the late Bruno Morando, who initially guided him in this work, for his support and assistance. This work is the result of a collaboration between many members of the different Consortia (INCA, FAST, NDAC, TDAC), it is a great pleasure to acknowledge their dedicated contribution. The author is supported by a research grant from the European Space Agency.

REFERENCES

Bange, J.-F., Bec-Borsenberger, A., 1997, ESA SP–402, this volume

Bastian, U., Wagner, K., 1997, *in* The Hipparcos and Tycho Catalogues, ESA SP–1200, Vol 4.

Bec-Borsenberger, A., 1985, *in* Scientific aspects of the Input Catalogue, ESA SP–234, 175

Bec-Borsenberger, A., Bange, J.-F., Bougeard, M.-L., 1995, A&A 304, 176

Dyson, F., 1928, Trans. IAU 3, 227

ESA, 1997, The Hipparcos and Tycho Catalogues, ESA SP–1200

Folkner, W.M., Charlot, P., Finger, M.H., et al., 1994, A&A 287, 279

Fienga, A., Arlot, J.-E., Pascu, D., 1997, ESA SP–402, this volume

Fricke, W., 1982, A&A 107, L13

Hestroffer, D., Mignard, F., 1997, *in* The Hipparcos and Tycho Catalogues, ESA SP–1200, Vol 3.

Hestroffer, D., Morando, B., 1995, *in* Future possibilities for astrometry in space. Joint RGO-ESA workshop, Cambridge, UK, 19-21 June 1995, ESA SP–379, 41

Hestroffer, D., Morando, B., Mignard, F., Bec-Borsenberger, A., 1995, A&A 304, 168

Høg, E., Makarov, V.V., 1997, *in* The Hipparcos and Tycho Catalogues, ESA SP–1200, Vol 4.

Kovalevsky, J., 1997, ESA SP–402, this volume

Kovalevsky, J., Lindegren, L., Perryman, M.A.C, 1997, *in* The Hipparcos and Tycho Catalogues, ESA SP–1200, Vol 3.

Lindegren, L., Froeschlé, M., Mignard, F., 1997, *in* The Hipparcos and Tycho Catalogues, ESA SP–1200, Vol 3.

Lindegren, L., Perryman, M.A.C, 1996, A&AS 116, 579

Mignard, F., Evans, D., van Leeuwen, F., 1997, *in* The Hipparcos and Tycho Catalogues, ESA SP–1200, Vol 3.

Morrison, L.V., Hestroffer, D., Taylor D.B., van Leeuwen, F., 1997, ESA SP–402, this volume

Viateau, B., Rapaport, M., 1997, this volume